Neuro-Oncology

Neuro-Oncology 16(11), 1484–1498, 2014
doi:10.1093/neuonc/nou102
Advance Access date 2 June 2014

Impact of meriolins, a new class of cyclin-dependent kinase inhibitors, on malignant glioma proliferation and neo-angiogenesis

Marie Jarry, Céline Lecointre, Céline Malleval, Laurence Desrues, Marie-Thérèse Schouft, Vadim Lejoncour, François Liger, Gildas Lyvinec, Benoît Joseph, Nadège Loaëc, Laurent Meijer, Jérôme Honnorat, Pierrick Gandolfo†, and Hélène Castel†

Inserm U982, Laboratory of Neuronal and Neuroendocrine Communication and Differentiation, Astrocyte and Vascular Niche, Biomedical Research Institute (IRIB), PRES Normandy, TC2N network, University of Rouen, Mont-Saint-Aignan, France (M.J., C.L., L.D., M.-T.S., V.L., P.G., H.C.); Neuro-oncology department, Hospices Civils de Lyon, Hôpital Neurologique, Bron, France (C.M., J.H.); Lyon Neuroscience Research Center INSERM U1028/CNRS UMR 5292, Lyon, France (C.M., J.H.); University of Claude Bernard - Lyon 1, Villeurbanne, France (C.M., J.H.); Institut de Chimie et Biochimie Moléculaires et Supramoléculaires UMR 5246, University of Claude Bernard - Lyon 1, Villeurbanne, France (F.L., G.L., B.J., N.L.); Protein Phosphorylation & Human Disease Group & USR3151, Station Biologique, Roscoff, France (N.L., L.M.); ManRos Therapeutics, Roscoff, France (L.M.)

Corresponding Author: Hélène Castel, PhD, Inserm U982, Laboratory of Neuronal and Neuroendocrine Communication and Differentiation, DC2N, Astrocyte and Vascular Niche, Biomedical Research Institute (IRIB), PRES Normandy, TC2N network, University of Rouen, 76821 Mont-Saint-Aignan, France (helene.castel@univ-rouen.fr).

†Indicates co-last authors.

Background. Glioblastomas are the most frequent and most aggressive primary brain tumors in adults. The median overall survival is limited to a few months despite surgery, radiotherapy, and chemotherapy. It is now clearly established that hyperactivity of cyclin-dependent kinases (CDKs) is one of the processes underlying hyperproliferation and tumoral growth. The marine natural products meridianins and variolins, characterized as CDK inhibitors, display a kinase-inhibitory activity associated with cytotoxic effects. In order to improve selectivity and efficiency of these CDK inhibitors, a series of hybrid compounds called meriolins have been synthesized.

Methods. The potential antitumoral activity of meriolins was investigated in vitro on glioma cell lines (SW1088 and U87), native neural cells, and a human endothelial cell line (HUV-EC-C). The impact of intraperitoneal or intratumoral administrations of meriolin 15 was evaluated in vivo on 2 different nude mice-xenografted glioma models.

Results. Meriolins 3, 5, and 15 exhibited antiproliferative properties with nanomolar IC_{50} and induced cell-cycle arrest and CDK inhibition associated with apoptotic events in human glioma cell lines. These meriolins blocked the proliferation rate of HUV-EC-C through cell cycle arrest and apoptosis. In vivo, meriolin 15 provoked a robust reduction in tumor volume in spite of toxicity for highest doses, associated with inhibition of cell division, activation of caspase 3, reduction of CD133 cells, and modifications of the vascular architecture.

Conclusion. Meriolins, and meriolin 15 in particular, exhibit antiproliferative and proapoptotic activities on both glioma and intratumoral endothelial cells, constituting key promising therapeutic lead compounds for the treatment of glioblastoma.

Keywords: cyclin-dependent kinase, glioma, meriolin, nude mice, tumor growth.

Brain tumors comprise only 1% of all cancers but contribute to 2.5% of overall cancer mortality and are the third leading cause of cancer death in young adults.[1] Malignant gliomas are the most common group of primary brain tumors, with an incidence of 8.9 cases per 100 000 persons/year in the United States.[2] These glial tumors represent a wide spectrum of malignancies ranging from slowly growing (low-grade astrocytoma) to highly aggressive glioblastoma (GBM) tumors[3] associated with very poor prognosis. Indeed, GBMs are highly vascularized and extremely invasive, conferring resistance to standard treatments (ie, surgery plus radiotherapy, eventually followed by chemotherapy).[4,5] The poor prognosis associated with GBM warrants continued intensive investigation of new therapeutic options, and rapid translation into clinical applications is an urgent necessity.

A hallmark of many human cancers is deregulation of cell-cycle progression affecting regulatory pathways and cellular

Received 27 August 2013; accepted 3 May 2014

processes such as proliferation, differentiation, DNA repair, and apoptosis leading to genetic instability, tumorigenesis, and malignancy.[6] Cell-cycle abnormalities are mainly due to hyperactivation of cyclin-dependent kinases (CDKs), members of the serine/threonine-specific protein kinase family, consisting of 20 members exhibiting conserved catalytic domains and similar activation mechanisms through the binding of a regulatory subunit (usually a cyclin) and post-translational modifications. Abnormal regulation of the CDK4- and CDK6-cyclin D-INK4-retinoblastoma protein (Rb) signaling pathway is among the most common aberrations found in many human cancers,[7] particularly GBM.[8–13] Recent profiling of molecular tumors has further highlighted the critical role of CDK4/CDK6 activation in the pathogenesis of GBM.[14,15] Taking account these observations, CDKs have since been extensively pursued as oncology drug targets among many other protein kinases with roles in cell cycle regulation.[16,17] Accordingly, depletion of either CDK1 or CDK2 slows down the progression through G2/M or G1/S, respectively, but combined depletion of CDK1 and CDK2 leads to much stronger G2/M arrest in the non-small cell lung cell line or apoptosis in osteosarcoma cells. In the same way, simultaneous inactivation of CDK1, CDK2, and CDK9 not only arrested cell cycle but also substantially induced apoptosis.[18] However, highly specific inactivation of any CDK, including CDK1, would not be as efficient as more broad inhibition of multiple CDKs. In addition, multitarget inhibitors may find appropriate medicinal use because they are less likely to allow development of resistance and may be more efficient. All CDK inhibitors identified to date are ATP competitive.[19] Many of them have been found to display promising antitumor activities, and a number are currently undergoing clinical evaluation as anticancer drugs.[20–22]

New synthetic 3-((2-amino)pyrimidin-4-yl)-7-azaindole CDK inhibitors, meriolins, are hybrid molecules derived from meridianins, a family of 3-((2-amino)pyrimidin-4-yl)indoles, and variolin B containing a central pyrido[3′,2′:4,5]pyrrolo[1,2-*c*]pyridine core substituted with a 2-aminopyrimidine ring.[23,24] Meridianins and variolin B are marine natural compounds that exhibit various levels of kinase inhibition and are extracted from the Ascidian *Aplidium meridianum*[25] and *Kirkpatrickia variolosa*, a rare Antarctic sponge,[26,27] respectively.[28,29] Recent studies established that variolin B and deoxyvariolin display CDK inhibition and antitumor activity,[30] whereas a first series of meriolins has shown potent inhibitory activities towards CDKs and antiproliferative and pro-apoptotic behaviors on human cancer cell lines in culture.[24] In particular, phosphorylation at CDK1-, CDK4-, and CDK9-specific sites has been shown to be counteracted by meriolins in neuroblastoma SH-SY5Y.[23] Meriolin 3 potently inhibited growth of Ewing's sarcoma and LS174T colorectal carcinoma xenografted into nude mice.[23] In the present study, the potential antitumoral activity of a new series of meriolin has been specifically evaluated on malignant glioma development, both in vitro and in vivo.

Materials and Methods

Compounds, Cell Lines and Culture Conditions

Meriolins were synthesized by Benoît Joseph's research group (ICBMS, University of Lyon) and provided by Dr. Laurent Meijer (ManRos Therapeutics). Meriolins were dissolved in dimethyl sulfoxide (DMSO) at a 10 mM stock solution and stored at −20°C.

Culture of Cell Lines

Human cell lines from anaplastic astrocytoma (SW1088) and glioblastoma (U87), human (HUV-EC-C), and murine (bEnd3) endothelial cell lines were obtained from the American Type Culture Collection. SW1088 cells were maintained in Leibovitz L-15 containing 10% fetal bovine serum (FBS; Lonza) and 1% sodium pyruvate at 37°C in a humidified atmosphere. U87 and bEnd3 cells were maintained in Dulbecco's modified Eagle's medium (DMEM; Invitrogen) containing 10% FBS and 1% sodium pyruvate at 37°C in a humidified atmosphere containing 5% CO_2. The HUV-EC-C cells were maintained in F12K (Invitrogen) containing 10% FBS, 1% sodium pyruvate, 0.1 mg/mL heparin, and 0.05 mg/mL endothelial growth factors (Invitrogen) at 37°C in a humidified atmosphere containing 5% CO_2. Culture media were replaced every 3 days.

Culture of Rat Astrocytes

Primary cultures of astrocytes were prepared as previously described.[30] Briefly, cerebella from 7-day-old (P7) Wistar rats were collected in DMEM/Ham-F12 (21, v/v%) culture medium supplemented with 2 mM glutamine, 1% insulin, 5 mM HEPES, 0.4% D(+)-glucose, and 1% of antibiotic-antimycotic solution. The tissues were disaggregated mechanically with a syringe equipped with a 1 mm gauge needle and filtered through a 100 μm pore-size mesh filter (Falcon; Becton Dickinson). Dissociated cells were resuspended in culture medium supplemented with 10% heat-inactivated FBS and seeded in 150-cm^2 culture flasks (Falcon) at a density of 20×10^6 cells/flask. Cells were incubated at 37°C in a humidified atmosphere (5% CO_2), and the medium was changed twice a week. When cultures were confluent, the flasks were gently shaken on an orbital shaker at 250 g for 2 hours. Dislodged cells were discarded, and a second step of purification was performed at 250 g for 14–16 hours. Remaining adhesive cells were collected by trypsination, centrifuged (800 g for 10 min) and plated in 150 cm2 flasks. Suspended astrocytes were harvested and seeded in 24-well poly-L-lysine-coated plates.

Culture of Neurons and Co-culture of Astrocyte-neuron

Cerebellar granule cell cultures were prepared from cerebella of P7 Wistar rats as described previously.[31] Isolated cells were plated on 14 mm culture dishes coated with poly-L-lysine (5 mM) at a density of 1.5×10^6 cells/dish and incubated at 37°C in a humidified atmosphere (5% CO_2) for 1 to 10 days before use. Culture medium consisted of DMEM/Ham's F12 (75%/25%) supplemented with 10% FBS, 2 mM glutamine, 5 μg/mL insulin, 25 mM KCl, and 1% of antibiotic-antimycotic solution. Culture of neurons and co-cultures were obtained by seeding granule cells (1.5×10^6 cells/mL) directly on fibronectine or astrocytes plated in 24-well plates after 12 hours. Co-cultures were maintained in the specific medium for neuron and incubated at 37°C in a humidified atmosphere (5% CO_2) for only 4 days.

Cell Growth Assay

SW1088, U87, HUV-EC-C, and bEnd3 cells were cultured in 24-well plates (Costar; 5×10^3 cells/well for SW1088 and HUV-EC-C, 15×10^3 cells/well for U87 and bEnd3) for 24 hours

before treatment in L-15, DMEM, DMEM, or F12K, respectively, supplemented with 10% FBS. Cells were then incubated in the absence or presence of graded concentrations of meriolins (10 pM to 10 μM) for 48h, 48h, 24h, and 72 h, respectively. Controls were determined by using a DMSO concentration corresponding to the dilution of meriolins used for each concentration tested. After treatment, cells were harvested, and cellular density was measured by direct cell counting with an electronic cell counter (Z2; Coulter Beckmann).

Cell Cycle Analysis

U87 and HUV-EC-C cell lines were plated in 75 cm^2 Falcon flasks. When cells reached 80% confluence, they were incubated in the absence or presence of meriolins 5 and 15 (0.1 μM) for 24 hours. Cells treated with DMSO corresponding to meriolin concentration were used as control. Cell cycle analysis was done by DNA staining with propidium iodide by flow cytometry. Briefly, after treatment, cells were trypsinized, harvested in PBS, and fixed in ice cold 70% ethanol for 2 hours. Staining was done with 0.6 mg/mL RNase (30 min; room temperature [RT]; Sigma-Aldrich) and 50 μg/mL propidium iodide (30 min; RT; Sigma-Aldrich). Cell cycle status was quantified by FacsCalibur flow cytometer (BD Biosciences) using CellQuest analysis software (Becton Dickinson Immunocytometry Systems).

Apoptosis Analysis Through Determination of $\Delta\Psi m$

SW1088, U87, and HUV-EC-C cell lines were plated in 25 cm^2 Falcon flasks. When cells reached 80% confluence, they were incubated in the absence or presence of meriolins 3, 5, 7, and/or 15 (0.1 μM) for 24 hours or 48 hours. Cells treated with DMSO corresponding to the meriolin concentration were used as control. Staurosporine treatment for 1 hour was used as a positive control. Changes in mitochondrial function induced by different apoptotic stimuli were associated with the mitochondrial membrane potential.[32] Damaged mitochondria lose membrane integrity and are not able to maintain their transmembrane potential as a consequence. Mitochondrial potential labeling, $\Delta\Psi m$, was determined by monitoring the fluorescence of the cationic potentiometric dye tetramethyl rhodamine methyl ester (TMRM). Briefly, after treatment, cells were harvested, rinsed in PBS, resuspended in a buffer containing 10 mM HEPES, 135 mM NaCl, 5 mM $CaCl_2$, and incubated 15 minutes in a fresh TMRM solution (200 nM, 37°C in the dark; Molecular Probes; Fischer Scientific). Red fluorescence was determined by FacsCalibur flow cytometer (BD Biosciences) in the FL2 channel at 575 nm using CellQuest analysis software. Representative results were shown as 2-dimensional density plots of TMRM-stained cells illustrating the percentage of cells with intact $\Delta\Psi m$ (TMRM fluorescence in top right quadrant).

Electrophoresis and Western Blotting

Following heat denaturation for 3 minutes, Sc1 cell proteins were separated on a minigel electrophoresis system (Invitrogen) using NuPage 10% Bis-Tris, 10- or 12-well polyacrylamide gels. Electrophoresis and transfer were performed in XCell SureLock Mini-Cell system and XCell II Blot module from Invitrogen. The 0.45 μm nitrocellulose membrane was from Fisher Bioblock. These were blocked for 1 hour with 5% low-fat milk in Tris-buffered saline-Tween-20, incubated overnight at 4°C, and analyzed by enhanced chemiluminescence. Monoclonal antibodies against actin were from Calbiochem. Monoclonal antibodies against Rb were purchased from BD Biosciences. Polyclonal antibody against phospho-Ser249/Thr252-Rb was provided by Biosource. Polyclonal antibody against phospho-Thr320-protein phosphatase 1α (PP1α) was from Cell Signaling. Polyclonal antibodies against RNA polymerase II and phospho-Ser2-RNA polymerase II were supplied by Covance Research Products. Polyclonal antibodies against PARP and against Mcl-1 were obtained from Santa Cruz Biotechnology.

Heterotopic Tumoral Growth Study

We used 2 different xenografted animal models to test the effect of meriolin 15 in vivo. Animal experiments were performed according to the recommendations of the French Ethical Committee and under the supervision of authorized investigators. First, we used U87 human glioblastoma cell line xenografted in nude mice. A cohort of 6–7-week-old male Swiss nude mice (Charles River Laboratory) was sedated by isoflurane inhalation (Aerane; Baxter) and implanted subcutaneously into the flanks with 3×10^6 U87 cells/100 μL PBS. During the protocol, tumor growth was evaluated every day. When tumors reached a volume of 100–150 mm^3, 100 μL of meriolin 15 or vehicle at the corresponding concentration were injected intraperitoneally (i.p.). A stock solution of 25 mg/mL in DMSO was prepared and stored at −20°C. In a first experiment, meriolin 15 was administrated at doses of 2 mg/kg every 2 days (meriolin 15, 2 mg/kg/2 d), 5 mg/kg every 2 days (meriolin 15, 5 mg/kg/2 d) or every day (meriolin 15, 5 mg/kg/d), diluted in DMSO in NaCl 0.9% (5/95, v/v%). In a second experiment, meriolin 15 was administrated at doses of 2.5 mg/kg twice daily (meriolin 15, 2×2.5 mg/kg), 5 mg/kg twice daily (meriolin 15, 2×5 mg/kg) or 10 mg/kg twice daily (meriolin 15, 5×10 mg/kg) diluted in polyethlyleneglycol (PEG)-300 in NaCl 0.9%. For the control, we injected mice with the same solutions but without meriolin 15. This model was used for ex vivo immunohistochemical investigation of proliferation, apoptosis, or vascular architecture. Thus, U87 tumor xenografts were collected, frozen in isopentane, and maintained at −80°C.

To confirm the observed effects on U87 human GBM cell line, we tested meriolin 15 on a second animal model. This model was developed in 2003 at the Neurology Department and Medical School of Vandoeuvre-lès-Nancy, France[33] using a piece of human GBM obtained after neurosurgical resection and grafted into nude mice (see details in Supplementary Materials and Methods). The obtained xenograft was maintained in nude mice by serial passages when tumors reached 1-2 cm^3. The day of xenograft was considered as day 0 (D0). At the onset of treatment, once tumors reached ∼250 $mm^3 \pm 40$ mm^3 in volume, mice were arbitrarily assigned to different groups ($n = 6$ to 8 each). Two independent experiments were conducted with intratumoral injection of meriolin 15 for 5 or 10 days. We tested different concentrations (2.5 mg/kg/day for 5 days,1.25 mg/kg/day for 5 days, 1.25 mg/kg/day for 10 days, and 1.8 mg/kg/day for 5 days). Meriolin 15 was diluted in 5% DMSO, 45% PEG, and 50% NaCl; for the control, we used as mice injected with the same solution without meriolin 15. During the 2 protocols, tumor growth

was evaluated every day, and animals were weighed every 2 days. The tumor volume was estimated according to its major and minor axes as measured with a slide caliper. Tumor volumes were calculated by assuming a spherical shape and using the formula: volume $= (a^2 \times A)/2$, where "A" and "a" are the long and short diameters, respectively. Mice were euthanized when the tumor volume reached 2 cm^3, and this day was considered as the survival time of the mice. Survival times were analyzed using the Kaplan-Meier method, and we also used the Wilcoxon statistical test to compare tumoral sizes.

Immunohistochemical Staining

Tumor sections (10 μm thick) were cut in a cryostat (Cryostat CM1950; Leica Microsystems), mounted on gelatin-coated slides, and maintained at −20°C until experiment. Briefly, slides were first rinsed in PBS, fixed in a paraformaldehyde solution (4%; 20 min; RT) and washed 3 times in PBS. Sections were permeabilized and preincubated in a PBS, Triton X100 0.3%, normal donkey antiserum NDS 1:50, and bovine serum albumin 0.5% solution (30 min; RT). Slides were then incubated with primary antibodies (4°C) (ie, anti-Ki67), -caspase 3, -collagen IV antibody (Santa Cruz Biotechnology), and anti-CD133 antibodies (1:200; overnight; Millipore). After treatment, slices were washed 3 times in PBS (10 min; RT) and incubated with corresponding secondary antibodies in a PBS/Triton 0.03% solution (1:300; 2 h; RT; in the dark). Finally, after washing, slices were incubated in 4′,6-diamidino-2-phenylindole dihydrochloride (DAPI; 1:1,000;10 min; RT; Sigma-Aldrich), washed again, and mounted in Mowiol 4–88 (Calbiochem). Tumor slices were then examined using a confocal microscope (Leica TCS SP2 AOBS). Quantitative analyses from the confocal acquisitions were calculated by using ImageJ 1.44. software.

Statistical Analysis

All statistical analyses were conducted using tGraphPad Prism 4.00 software (GraphPad Software). Data were expressed as mean values ± SEM of 3 or more separate experiments. Among the experiments, data were analyzed with different statistical tests (ie, Friedman test followed by Dunn' and Dunnett' multicomparison test [cell cycle, apoptosis, kinetic of tumor growth], Wilcoxon or Mann-Whitney tests [tumoral volume of heterotopic xenografts and mouse weight], Kruskal-Wallis test [quantification of immunohistochemical labeling], or the Cox-Mantel log-rank test (survival).

Results

Selected Meriolins Inhibit Human Glioma Cell Growth in Vitro

We explored the antitumoral activity of various meriolins on 2 human glioma cell lines (ie, anaplastic astrocytoma [SW1088] and human glioblastoma [U87]). Both cell lines were exposed to increasing concentrations yielding dose-dependent proliferation rate inhibition after 48 hours of treatment. IC50 values indicated that 19 meriolins efficiently decreased cell growth in a concentration range from 1 nM to 1 μM (data not shown). Among them, meriolins 3, 5, and 15, whose structures are illustrated in Figure S1, showed an interesting reduction of more than 70% of the proliferation rate of both glioma cell lines with IC50 values of 34, 32, and 46 nM, respectively, for SW1088 (Fig. 1A) and of 76, 18.4, and 5.1 nM, respectively, for U87 (Fig. 1B). Conversely, meriolin 7, which presents a modified irrelevant structure (Fig. S1), was devoid of antiproliferative activity (Fig. 1A and B). The cytotoxic effect of meriolins was also tested on primary proliferating astrocyte and neuron cultures as well as astrocyte-neuron co-cultures from 7-day-old cerebellum rat pups. Meriolins 5 and 15 still showed antiproliferative and pro-death activities, yielding IC50 values for meriolin 15 of 7.8 nM in astrocytes and 4.7 nM in neurons (Fig. 1C, left and middle panels). An important feature of this study was that the astrocytes remained more quiescent, whereas neurons started differentiating in the astrocyte-neuron co-cultures.[34,35] In these less proliferating and more differentiating co-cultured native cells, meriolins 5 and 15 exhibited lower activities than in glioma cells (Fig. 1C, right panel).

Meriolins Induce Arrest of Cell Cycle and Promote Apoptosis of Human Glioma Cell Lines

The cell cycle distribution of the U87 glioblastoma cell line was examined using flow cytometry with propidium iodide in the absence or the presence of meriolins 5 and 15 (0.1 μM each) (Fig. 2A). As illustrated in Figure 2A and B, after a 48 hour exposure with meriolins 5 and 15, the G1 phase appeared significantly reduced ($P < .01$), whereas the G2/M phase markedly increased compared with control ($P < .05$). No significant sub-G1 accumulation could be observed after 48 hours of treatment (Fig. 2B). In addition, systematic cell cycle analysis revealed a progressive accumulation of cells in the diploid phase of the cycle with both meriolin 5 and meriolin 15 (data not shown). The meriolin 15-induced morphological changes and cell cycle arrest would be accompanied by cell death events potentially including delayed apoptotic and nonapoptotic mechanisms. One of the initial events of mitochondrial alteration is a decreased mitochondrial membrane potential $\Delta\Psi m$, likely detectable by loss of the orange/red fluorescence of the fluorescent dye TMRM, as described in the Materials and Methods section. In representative 2-dimensional density plots of TMRM-stained cells illustrating percentage numbers of still-alive cells with intact $\Delta\Psi m$ (TMRM fluorescence in top right quadrant), it was shown that 24 hour exposure of SW1088 and U87 to meriolins 5 and 15 (0.1 μM, each) increased cell death and remaining healthy cells decreased from 70% to 51% and 44% in SW1088 and from 77% to 67% and 71% in the presence of meriolins 5 and 15, respectively (Fig. 3A); however, only the effect of meriolin 5 (SW1088) was significant at 24 hours (Fig. 3B, $P < .05$). In U87, the effect of meriolins 5 and 15 was moderate at 24 hours and marked at 48 hours (Fig. 3A). In both glioma cell lines, the proapoptotic agent staurosporine (0.1 μg/mL; 1 h) induced loss of $\Delta\Psi m$ in glioma cells, whereas no change occurred with meriolin 7 (Fig. 3A). These data suggest that meriolins 5 and 15 induce astrocytoma and glioblastoma cell-cycle arrest in G2/M phase and loss of mitochondrial potential, reflecting apoptosis and/or nonapoptotic cell death that likely contribute to the inhibition of proliferation and glioma cell death in vitro.

We also analyzed the effects of meriolin 15 on various markers in human GBM Sc1 cells (Fig. 4). Sc1 cells were exposed to 65 nM meriolin 15 (corresponding to 3 times the IC50 value for meriolin

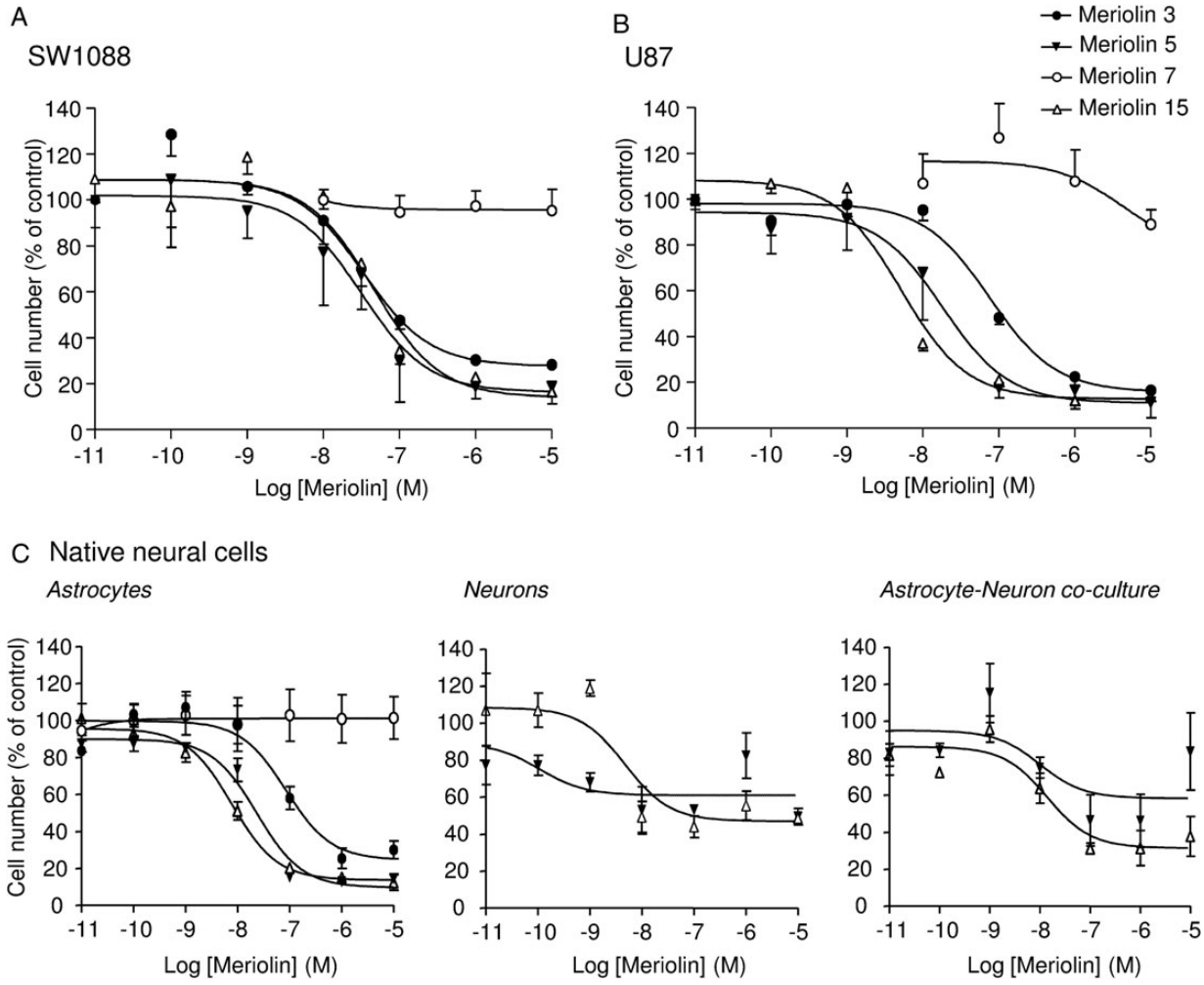

Fig. 1. Antiproliferative effect of selected meriolins on human glioma cells and native astrocytes and neurons in vitro. (A and B) Human anaplastic astrocytoma cells SW1088 (A) and human glioblastoma cells U87 (B) were incubated for 48 hours with graded concentrations of meriolin 7 (10 nM to 10 μM) or meriolins 3, 5, and 15 (10 pM to 10 μM) and counted using a Coulter counter. (C) Rat native neonatal astrocytes (left) were treated for 48 hours with graded concentrations of meriolins 3, 5, 7, and 15 (10 pM to 10 μM), whereas neurons (middle) or astrocytes and neurons in co-culture (right) were treated for 48 hours with meriolins 5 and 15 (10 pM to 10 μM) and then counted using the Coulter counter. The active and potent meriolins 3, 5, and 15 induced growth inhibition in tumoral cells but also in native neural cells, which were mostly proliferating. Data are mean of 3 to 9 independent experiments performed in triplicate.

15 on this cell line) for increasing durations (1.5 h to 24 h). Cells were then collected, and proteins were extracted and resolved by SDS-PAGE, followed by analysis by Western blotting with various antibodies. Meriolin 15 induced downregulation of the survival factor Mcl-1, caspase 3, RNA polymerase II, and PARP cleavage as well as dephosphorylation of the CDK1/CDK2/CDK7/CDK9 sites on protein phosphatase 1α (Thr320), RNA polymerase II (Ser 2), and Rb (Ser249/Thr252, Ser807/Ser811). These results confirm the direct effect of meriolin 15 on endogenous CDKs, leading at least in part to the activation of an apoptotic pathway.

Meriolins Inhibit Cell Growth, Arrest Cell Cycle, and Induce Apoptosis of Endothelial Cells

Growth and expansion of high-grade glioma tumors are associated with vascular endothelial cell proliferation and migration, leading to lumen formation referred to as neoangiogenesis. Thus, because meriolins exhibited antimitogenic activity on glioma cells, we also investigated their potential role on transformed human (HUV-EC-C) and mouse (bEnd3) endothelial cell lines. In the presence of the corresponding concentration of DMSO (as control) or meriolin 7, HUV-EC-C cells exhibited elongated forms, whereas relevant proapoptotic morphological changes and cell detachment have been observed in the presence of meriolin 15. A 72 hour treatment with meriolins 3, 5, or 15 at a concentration of 0.1 μM decreased the growth of the HUV-EC-C endothelial cells by 29.5%, 42.5%, and 58.2%, respectively (Fig. 5A). Similar meriolin-inducing cell death has been detected on the murine bEnd3 cell line with IC_{50} values in the micromolar range (Table S1; Fig. S2). We analyzed the effect of the most efficient meriolins (5 and 15) on the cell cycle profile of HUV-EC-C cells. In the representative example, only meriolin 15 (24 h) caused G2/M phase arrest and retention, with the G2/M

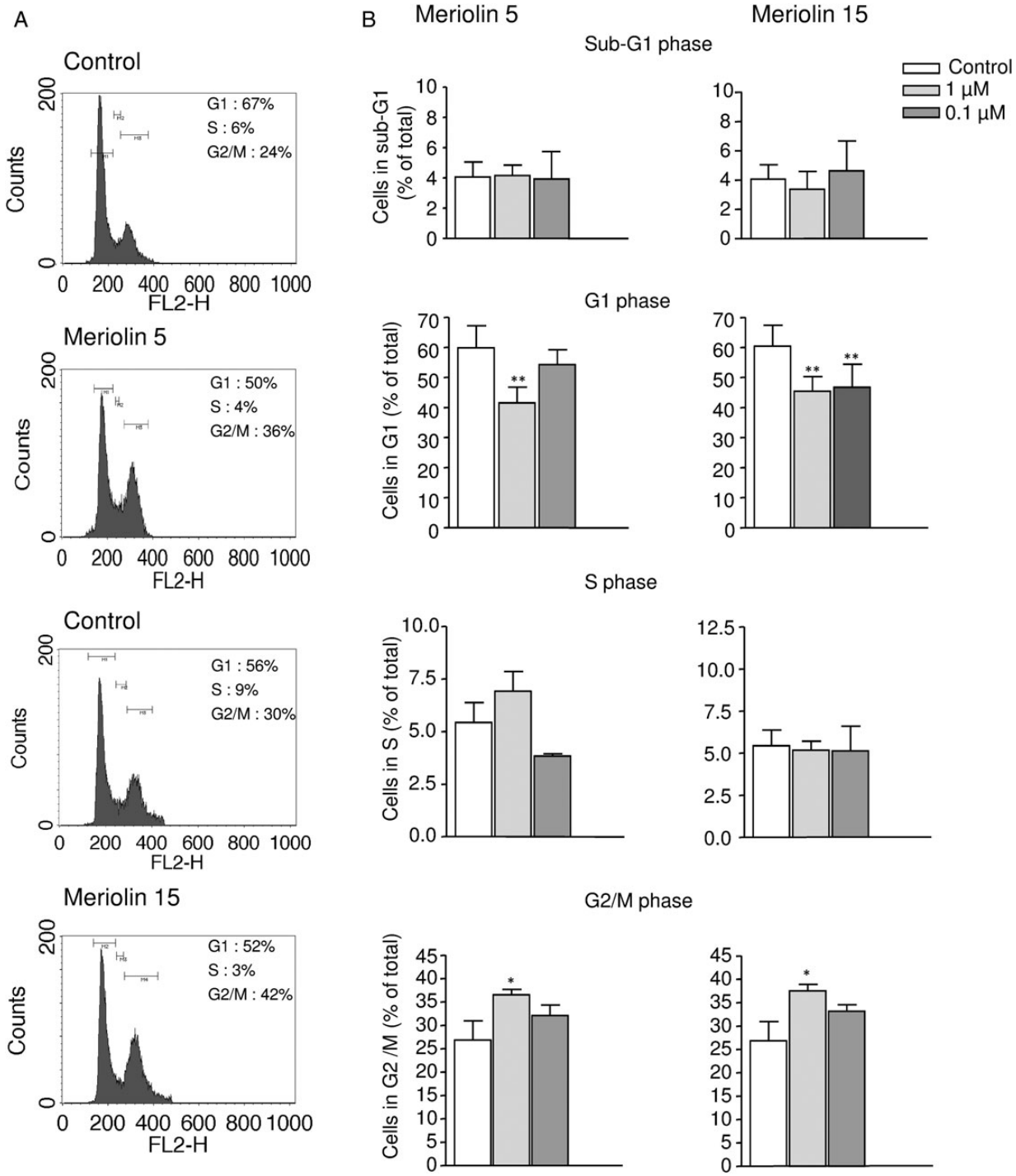

Fig. 2. Meriolins 5 and 15 arrested cell cycle in G2/M phase. (A) Representative effect of meriolins 5 and 15 (0.1 μM) on U87 cell cycle after 24 hour treatment. Cell cycle analysis following propidium iodide intercalation into the cellular chromatin was performed by flow cytometry. Data are representative of relative fluorescence intensity of G1, S, and G2/M-phase populations in a 2-dimensional FACS profile. The percentage of cells in each phase is indicated. (B) Bar graph of the percentage of U87 cells in G1, S, and G2/M phases after 24 hour treatment with DMSO 0.1% (control) and meriolins 5 and 15 (0.1 μM and 1 μM) in culture medium. Statistical significance was determined using 1-way ANOVA test followed by the Dunnett' post test. *$P < .05$; **$P < .01$, meriolin 5 or 15 (1 and 0.1 μM) versus. control group.

population increasing from 15% for control cells (DMSO) to 21% (meriolin 15, 0.1 μM) (Fig. 5B). Accordingly, the population in S phase decreased from 6% to 2% without significant modification of G1 phase after 24 hours of treatment. As already described in glioma cells, we did not observe an increase in the sub-G1 fraction of meriolin 15-treated HUV-EC-C cells. To analyze the

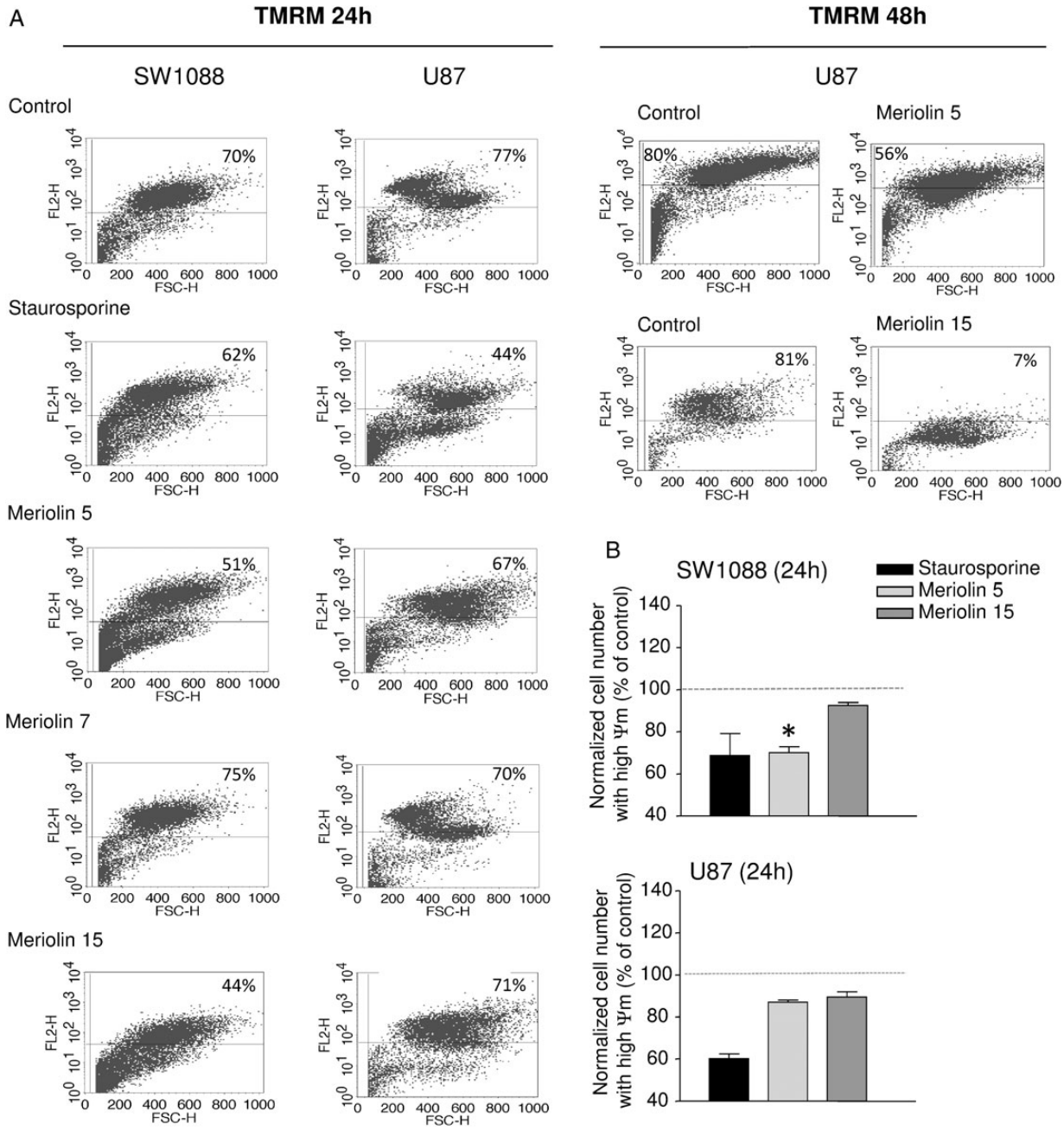

Fig. 3. Meriolins 5 and 15 induced loss of mitochondrial potential. Apoptotic events were determined through characterization of the changes in mitochondrial membrane potential $\Delta\Psi$m as revealed by the orange/red decrease of TMRM labeling. Results are shown as color-enhanced density dot plots, and values in upper right quadrants indicate percentage of viable cells with intact $\Delta\Psi$m. (A, left) SW1088 and U87 cells were treated for 24 hours in the absence or presence of meriolins 5, 7, and 15 (0.1 μM, each) or the validated proapoptotic agent staurosporine (1 μg/mL, 2 h). Right, U87 cells were also incubated with meriolins 5 and 15 during 48 hours and exhibited drastic loss of $\Delta\Psi$m. (B) Quantification of the effect of meriolins 5 and 15 on SW1088 and U87 cell number with intact $\Delta\Psi$m. The data are presented as mean ± SEM from 3 independent experiments. Statistical significance was determined using the 1-way ANOVA test followed by the Dunnett' post test. *$P < .05$; meriolin 5 (0.1 μM) versus control group.

mechanisms involved in inhibition of cell proliferation, we examined $\Delta\Psi$m change in HUV-EC-C with TMRM fluorescence. As depicted by the orange/red TMRM labeling, the majority of untreated (DMSO) or meriolin 7-treated endothelial cells (95%) were viable (Fig. 5C). In contrast, staurosporine (0.1 μg/mL; 1 h), meriolins 5 and 15 (0.1 μM each; 24 h) led to cell integrity loss of 88%, 65%, and 59% as illustrated by a diminished number of TMRM-labeled cells in the right quadrant (Fig. 5C). Our findings demonstrated that meriolins 5 and 15 have markedly stopped human endothelial cell proliferation by arresting cell cycle

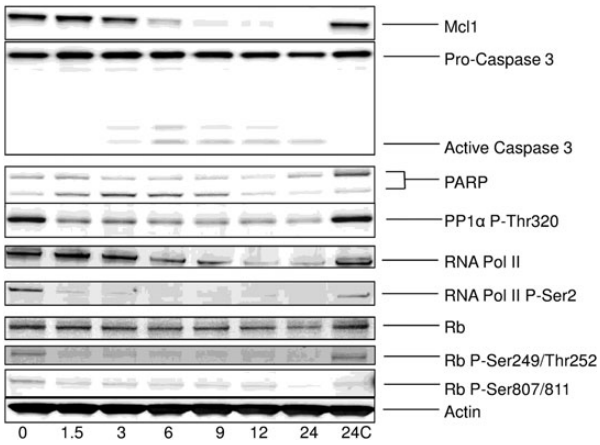

Fig. 4. Meriolin 15 inhibited endogenous CDKs and activated apoptosis in human GBM Sc1 cells. Sc1 cells were treated with 65 nM ($3 \times IC_{50}$) meriolin 15 for increasing durations (0 h–24 h). Cell proteins were extracted and resolved by SDS-PAGE followed by analysis by Western blot with antibodies directed Mcl-1, caspase 3, Poly-ADP ribose polymerase (PARP), phospho-Thr320 protein phosphatase 1α (PP1 α P-Thr320), RNA polymerase II (RNA Pol II), phosho-Ser2 RNA polymerase II (RNA Pol II P-Ser), Retinoblastoma protein (Rb), phospho-Rb Ser249/Thr252, Ser807/Ser811 (Rb P-Ser249/Thr252), and P-Ser807/811). Actin was used as a loading control. Some cells (24C) were exposed to DMSO vehicle only for 24 hours.

progression and exhibed proapoptotic/cell death activities in both tumoral glioma and endothelial cells. Thus, the most efficient meriolin, 15, has demonstrated effects on glioma growth, cell cycle arrest, and apoptosis/nonapoptotic death in endothelial and glioma cells, which makes it a promising candidate to optimize for treatment of high-grade glioma.

In Vivo Antitumoral Activity of Meriolin 15 on GBM Growth in Nude Mice

To investigate whether inhibition of CDKs by meriolins leads to tumor regression, meriolin 15 was administrated i.p. in nude mice xenografted with human glioblastoma U87 cells (Fig. 6A and B) or intratumorally in other nude mice xenografted with human GBM Sc1 (Fig. 6C–F). In the set of U87 xenografts, meriolin 15 significantly slowed glioblastoma growth at a dose of 5 mg/kg, compared with the vehicle group (corresponding DMSO dilution in NaCl 0.9%) when administered daily (Fig. 6A). In particular, an 8-day treatment with meriolin 15 led to about 50% (2 mg/kg/2d), 40% (5 mg/kg/2d), or 60% (5 mg/kg/d) inhibition of tumor growth in vivo, with mean tumor volume values of 998 ± 294 mm^3 in vehicle (DMSO) and 446 ± 42 ($P < .05$), 603 ± 114 and 362 ± 95 mm^3 ($P < .05$) under meriolin 15 treatments, respectively. No systemic toxicities, such as food and water consumption or spontaneous activity, were detected in these animals, and mice weight gains were not significantly different between vehicle- and meriolin-treated groups (Fig. S3A). In order to enhance meriolin 15 doses, taking into account the insolubility above 5 mg/mL, meriolin 15 was diluted in PEG-300 and administered i.p. twice a day from 2.5 mg/kg to 10 mg/kg to reach optimum tumor cytotoxicity. At 5 mg per day (2×2.5 mg/kg), meriolin 15 exhibited a very similar inhibitory effect on glioblastoma tumor growth during 14 days of treatment (Fig. 6B). Again, the mean tumor volume 8 days after the first meriolin injection was significantly lower in the meriolin-treated mice ($P < .01$), but mouse survival was not significantly enhanced. However, when 10 mg/kg and 20 mg/kg were administered daily, animals exhibited drastic weight loss (Fig. S3B) and death after 8 and 2 days of treatment, respectively. Thus, these data showed that meriolin 15 delays tumor growth after systemic administration but induces animal toxicity at high doses.

To confirm the efficacy of meriolin 15 in vivo, we tested an intratumoral injection procedure using 2.5 mg/kg/day during 5 days on human GBM Sc1. We observed significant inhibition of the tumor growth (Fig. 6C, $P < .05$) and increase of the overall survival compared with the PEG-DMSO vehicle ($P = .02$; Fig. 6D), and 3 of the 7 treated mice were totally cured. However, at this dose we observed an important inflammatory cutaneous reaction, which was associated with a local necrosis, in all treated mice. To avoid this toxic effect, we tested 1.8 mg/kg/day during 5 days and 1.25 mg/kg/day during 10 days. No local inflammatory reaction was detected with these protocols, and tumor growth was significantly delayed (Fig. 6E). Significant differences in mouse survival were observed with the 1.25 mg/kg/day dose during the 10 day schedule ($P = .051$ or 1.8 mg/kg/day during 5 days ($P = .015$) compared with vehicle, where there were no cured mice (Fig. 6F).

Analysis of in Vivo Antitumoral Effect of Meriolin 15

U87-bearing tumor sections were examined for the effect of i.p. administered meriolin 15 (Fig. 7A) on proliferation, differentiation, and/or apoptosis/cell death. Immunohistochemical analysis showed that the rate of cell division within the tumor, as revealed by labeling of the proliferation marker Ki67, significantly decreased by 36.6% after treatment with 2 mg/kg/2day (Fig. 7A). This mechanism was correlated with the enhanced activity of caspase 3 (Fig. 7B). In addition, the expression of CD133, the marker for tumoral stem cells or undifferentiated cells, was significantly inhibited by 86.05% in tumor sections extracted from meriolin 15-treated mice (5 mg/kg/d) (Fig. 7C). We also tested whether tumor cell death was tightly coupled to blood vessel regression and measured the number of vessels. Interestingly, analysis of the vascular basement membrane through collagen IV immunolabeling indicated that the basement membrane did not disappear but rather showed thin strands of basement membrane, the number of which number decreased significantly after (5 mg/kg) of meriolin 15 (Fig. 7D) accompanied by large blood lakes. These data indicate that a systemic treatment with meriolin 15 inhibits cell proliferation, reduces the number of undifferentiated cells and vascular components, and induces cell death at least in part via a caspase-3-dependent apoptotic pathway.

Discussion

We investigated the potential antitumoral effects of a series of meriolins designed as synthetic hybrid molecules between 2 different classes of marine natural products named meridianins (extracted from an ascidian) and variolins (extracted from a sponge), which have been previously characterized as kinase/CDK inhibitors and antitumoral agents.[24,28,29] A first set of meriolins

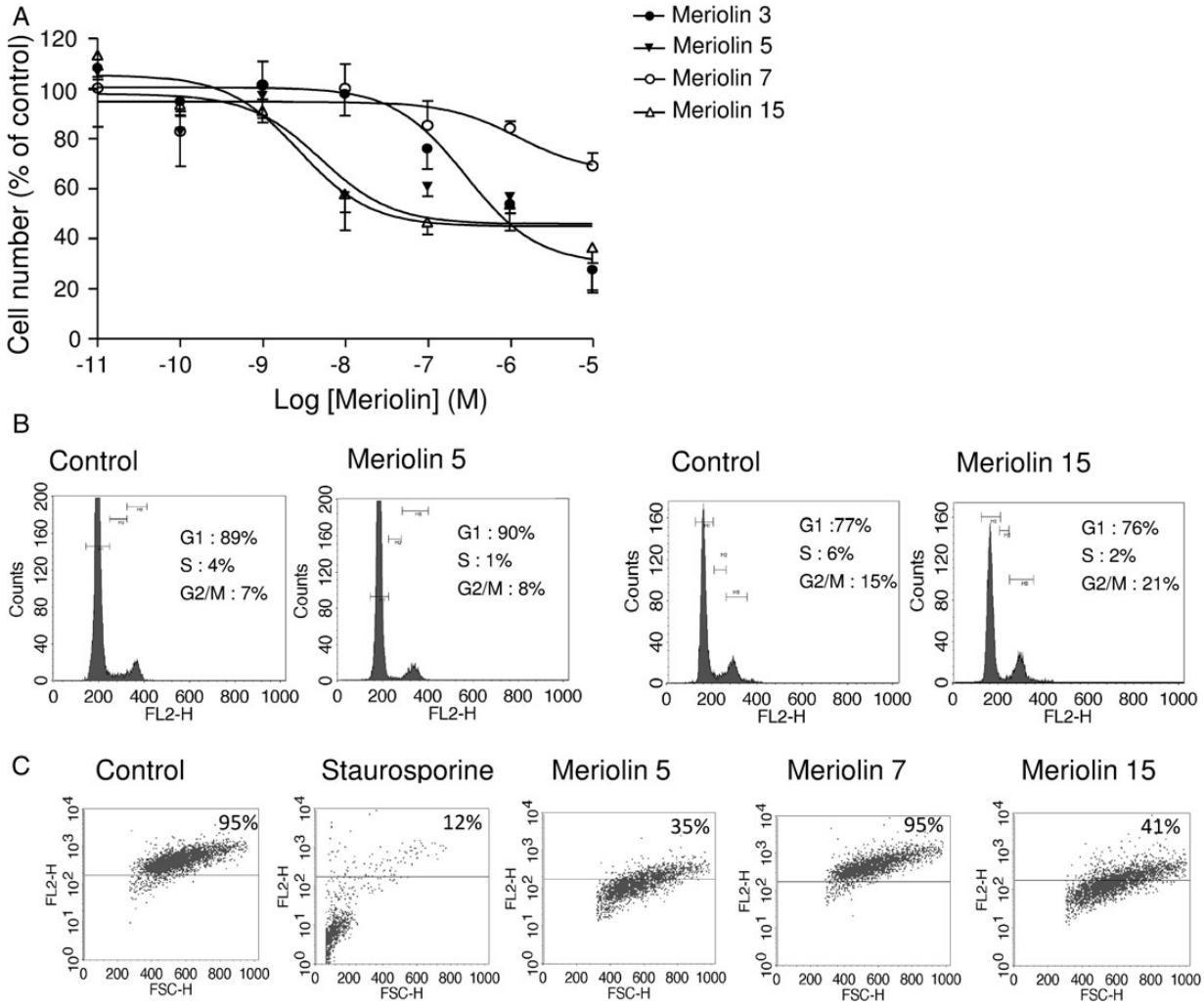

Fig. 5. Meriolins 3, 5, and 15 inhibited cell growth, arrested cell cycle in G2/M phase, and induced apoptosis of human endothelial cells in vitro. (A) Effect of increasing concentrations (10 pM to 10 μM) of meriolins 3, 5, 7, or 15 on the number of human endothelial cells HUV-EC-C. (B) Effect of meriolins 5 and 15 (0.1 μM, 72 h) on HUV-EC-C cell cycle by analysis of DNA content by FACS. Cell population decreased in S phase and increased in G2/M, as indicated on the graph. (C) Evaluation of changes of $\Delta\Psi$m in the absence or presence of meriolins 5, 7, and 15 (0.1 μM each, 24 h) or staurosporine (0.1 μg/mL, 1 h) through FACS analysis of TMRM labeling represented as color-enhanced density plots. Values indicate percentage cells with intact $\Delta\Psi$m after treatment with meriolins 5, 7, and 15 in a representative experiment.

(meriolins 1–14) was synthesized, and previous data indicated that some of them induced cell death in 5 tumorigenic or transformed cell lines: neuroblastoma SH-SY5Y, HEK293, glioma GBM cells in primary culture, multiple myeloma KMS-11, and colorectal adenocarcinoma LS1746T cell lines.[24] We tested the ability of variolin B and different meriolins to affect SW1088 anaplastic astrocytoma and U87 glioblastoma cell growth. Among the many compounds tested, some were clearly inactive, including meriolin 7, and others were more efficient than variolin B (IC_{50} values from 1 nM to 1 μM); meriolins 3, 5, and 15 exhibited the higher potency with nanomolar IC_{50} values. The co-crystallization of variolin B or meriolin 5, interacting with CDK2/cyclin A, showed a different orientation of these 2 inhibitors in the ATP-binding pocket of CDK2.[24] This observation may at least in part explain the increased efficiency of the meriolin family on CDK2 inhibition and consequently on glioma cell growth. In addition, increased meriolin efficiency would also result from the target preference for kinases. Indeed variolin B has been reported to inhibit CDK1, CDK2, CDK9, FLT3,[23] and to a lesser extent, CDK7,[29] whereas some meriolins have exhibited preference for CDK1, CDK2, CDK4, and CDK9.[24] Thus, targeting CDK4 may provide a key advantage for meriolins in the treatment of malignant glioma.

In our study, we demonstrated that meriolins 5 and 15 showed the most potent antiproliferative effect on both astrocytoma and GBM cells in vitro. We also investigated whether the susceptibility to meriolins was specific for the neoplasic phenotype of glioma cells or if it could be observed in untransformed isolated rat astrocytes and neurons as well as astrocytes and neurons in co-culture. Treatment at different doses of meriolins 5 and 15 resulted in astrocytic and immature neuron detachment and death. When these neural cells were co-cultured, likely leading to a reduced proliferation rate of astrocytes and pro-differentiation of neurons,[34,35] the toxic effects of meriolins appeared to be a lesser degree than in glioma cells. The lack of

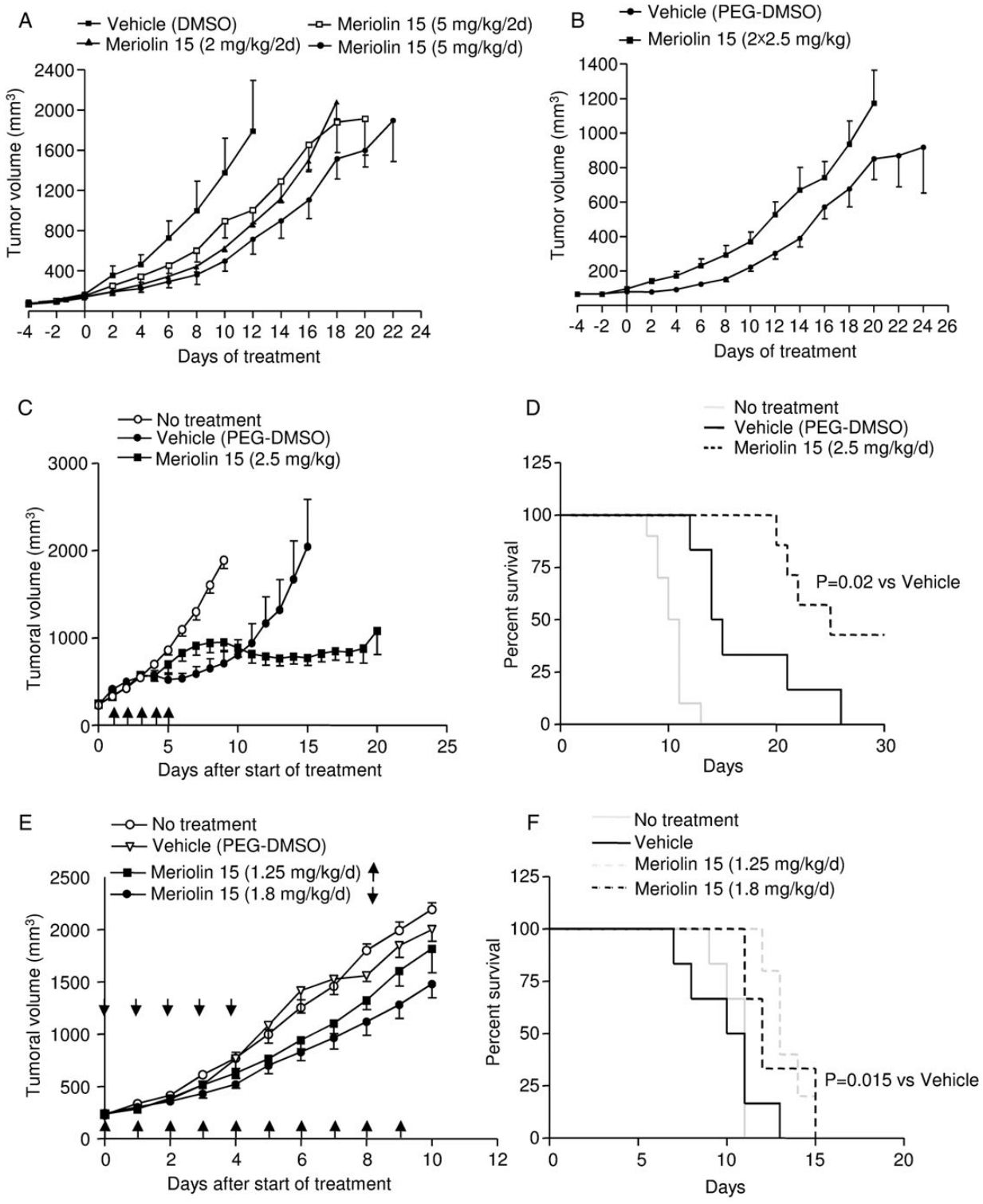

Fig. 6. Inhibitory role of meriolin 15 on U87 and human GBM sc1 xenograft development in nude mice. (A and B) U87 cells (3×10^6 cells, 100 μL PBS) were implanted subcutaneously into the right flanks of nude mice. (A) When tumors reached a volume of ~100–150 mm^3, mice were treated i.p. every 2 days with meriolin 15 (2 mg/kg/2d, $n = 4$) or (5 mg/kg/2d, $n = 5$) or every day (5 mg/kg/d, $n = 4$) or with vehicle (DMSO in NaCl 0.9%, $n = 4$) during 22 days. Statistical significance was determined by the Freidman test followed by the Dunn' multiple comparison test. *$P < .05$, meriolin 15 (2 mg/kg/2d) group versus vehicle group. #, $P < .05$, meriolin 15 (5 mg/kg/d) group versus vehicle group. (B) Mice were treated intraperitoneally twice a day every day with meriolin 15 (2×2.5 mg/kg/2d, $n = 9$), (2×5 mg/kg/2d), (2×10 mg/kg), or vehicle (PEG-DMSO, $n = 8$) during 24 days. Statistical significance was

specificity for the neoplastic phenotype of glioma cells may be attributed, on one hand, to the proliferating behavior of normal astrocytes (or immature neurons in culture) and, on the other hand, to pro-death/apoptotic function, likely predicting neurotoxicity.

In glioma, meriolin 15 diminished the number of cells in the S phase and increased the cell proportion in the G2/M phase, triggering cell cycle arrest. It was noted that no sub-G1s were clearly visible in cell cycle experiments, which suggested no DNA fragmentation (a hallmark of apoptotic cells), whereas meriolin15 induced caspase-3 activation and PARP cleavage. It has been previously suggested that apoptotic cells in which DNA degradation is terminated at 50–300 kb fragments and does not proceed to internucleosomal-size fragments,may not be identified as sub-G1 cells.[36] However, we also found that meriolins 3, 5, and 15 initiated cell death hallmarks, such as cell cycle arrest and decrease in the mitochondrial membrane potential $\Delta\Psi$m revealed by the fluorescent shift of TMRM.[37] Indeed, although apoptosis is the best characterized form of programmed cell death, nonapoptotic forms of cell death, referred as programmed cell death II (autophagy) or III (oncosis) independent of caspase activation and chromatin condensation, are now recognized as playing significant roles in cancer regression.[38,39] It has been shown that apoptosis and oncosis, a prelethal process that occurs in ATP-depleted cells,[40] have some features in common, such as the mitochondrial permeability transition and loss of $\Delta\Psi$m. In addition, we observed that meriolin-treated cells underwent morphological changes (ie, retraction and rounding) that have been previously associated with cell injury and widespread cytoskeletal framework disruption[41] resembling oncosis-associated morphological change.[40] Furthermore, cells showed a visible reduction of ability to adhere and spread, suggesting a loss in cell matrix adhesion.[42] Then, nonapoptotic oncosis cell death associated with cell and organelle swelling and swollen nuclei may also occur after meriolin 15 treatment, simultaneously developing with apoptosis in glioma. The cellular swelling accompanying oncosis, which is characterized by release of inflammatory signals[43,44] and stimulation of cell-mediated immunity,[45] may explain at least in part the necrotic features of the GBM sc1 tumors after intratumoral injections of meriolin 15. Together, we propose that meriolin 15, via potent inhibition of cyclin-dependent kinases by occupying the ATP binding site of enzymes' catalytic subunits, activates the intrinsic apoptotic pathway and nonapoptotic cascades that lead to necrosis.

Thus, it is proposed that meriolins and, more particularly, meriolin 15 inhibit CDK7/CDK9 and consequently decrease RNA polymerase II and its phosphorylation and lead to downregulation of the survival factor Mcl-1 (Fig. 4), thereby allowing the activation of proapoptotic factors (Noxa, Bim, etc.). These mechanisms likely explain the mitochondrial membrane potential changes and caspase 3-dependent activation of apoptosis that are observable in vitro and in vivo. A similar CDK7/CDK9 – RNA polymerase II – Mcl-1 – apoptosis sequence has been described in detail for the action of roscovitine and S-CR8.[46,47] Moreover, the disruption of cell cycle progression, both at the G1/S and G2/M transition, would result from inhibition of CDK1 and CDK2 and allow E2F1-dependent apoptosis.[48] Recent genetic evidence that mice survive in the absence of all interphase CDKs suggests that CDK1 is the critical kinase and that it is able to substitute missing activity of any other CDKs. In addition, Shapiro demonstrated the significance of only CDK1, CDK2, and CDK9 for cell cycle and viability.[18] The ability of meriolins to block cell cycle and induce apoptosis in glioma regardless of their p53 status and CDK mutations[49] is thus probably due to the combined CDK1, CDK2, and CDK9 inhibition mechanisms. From this observation, it appears that highly specific inactivation of any CDK would not be as efficient as broader inhibition of multiple CDKs as long as it includes CDK1. From this point of view, meriolins constitute a promising new CDK-inhibitor family with significant antitumoral activity on the most malignant glioma.

Besides the direct effects of oncogenic changes on cell proliferation and survival, the genomic alterations that occur during cancer progression are known to promote invasion and neoangiogenesis. An important factor underlying this phenotype is enhanced VEGF expression, which is commonly observed in malignant glioma.[50] Several existing CDK inhibitors have been shown to influence angiogenesis. For example, the potent selective CDK inhibitor SNS-032 prevents migration of HUVECs and reduces formation of a capillary network from these cells in culture.[51] Here, meriolins 3, 5, and 15 significantly decreased the endothelial cell HUV-EC-C proliferation rate, slowed the progression through G2/M and G1/S, and drastically initiated apoptosis/mitochondrial dysfunction. Connections between angiogenesis, mRNA transcription, and CDK9 have been previously suggested. Indeed, some CDK inhibitors (including flavopiridol, SNS-032, and roscovitine), which are currently under clinical evaluation as anticancer drugs, have also been shown to inhibit angiogenesis in vitro,[51–54] whereas they all share significant activity on CDK9. Thus, the effects of meriolins on endothelial cells are probably mediated by inhibition of CDK1/2 (cell cycle arrest) and CDK9 (apoptosis), leading to antimitogenic and cytotoxic activities. Considering the

determined by a Mann-Whitney test. $^{**}P < .01$, meriolin 15 (2 × 2.5 mg/kg/d) group versus vehicle group, $^{***}P < .001$, meriolin 15 (2 × 2.5 mg/kg) group versus vehicle group. (C–F) Inhibitory role of meriolin 15 on human GBM sc1 xenograft development in nude mice. GBM Sc1 fragments were implanted subcutaneously into the right flanks of nude mice. (C) Once tumors reached ~250 mm^3 in volume, mice received no injection or intratumoral injection of meriolin 15 (2.5 mg/kg, $n = 7$) or vehicle (PEG-DMSO, $n = 6$) during 5 days as indicated by black arrows. Statistical significance was determined by the Mann-Whitney test. $^{**}P < .01$, meriolin 15 (2.5 mg/kg) groups versis vehicle (PEG-DMSO) group. Statistical significance was determined by the by the Friedman test, followed by the Dunn' multiple comparison test. $P = .3$, meriolin 15 (1.8 mg/kg) groups versus vehicle group. (D) Kaplan-Meier survival rates of nude mice with flank xenografted GBM Sc1 for each of the treatments described in C. Statistical significance was determined by the log-rank test. $P = .02$, meriolin 15 (2.5 mg/kg/d) group versus vehicle group. (E) Mice received no injection or intratumoral injection of meriolin 15 in vehicle (1.8 mg/kg, $n = 6$), (1.25 mg/kg, $n = 5$) or vehicle (PEG-DMSO, $n = 6$) during 5 days or 10 days, respectively, as indicated by black arrows. Statistical significance was determined by the Friedman test followed by the Dunn' multiple comparison test. $^{*}P < .05$, meriolin 15 (1.8 mg/kg) groups versus vehicle group. (F) Kaplan-Meier survival rates of nude mice with GBM Sc1 flank xenografts for each of the treatments described in E. Statistical significance was determined by the log-rank test. $P = .051$, meriolin 15 (1.8 mg/kg/d) and $P = .015$, meriolin 15 (1.8 mg/kg/d) groups versus vehicle group.

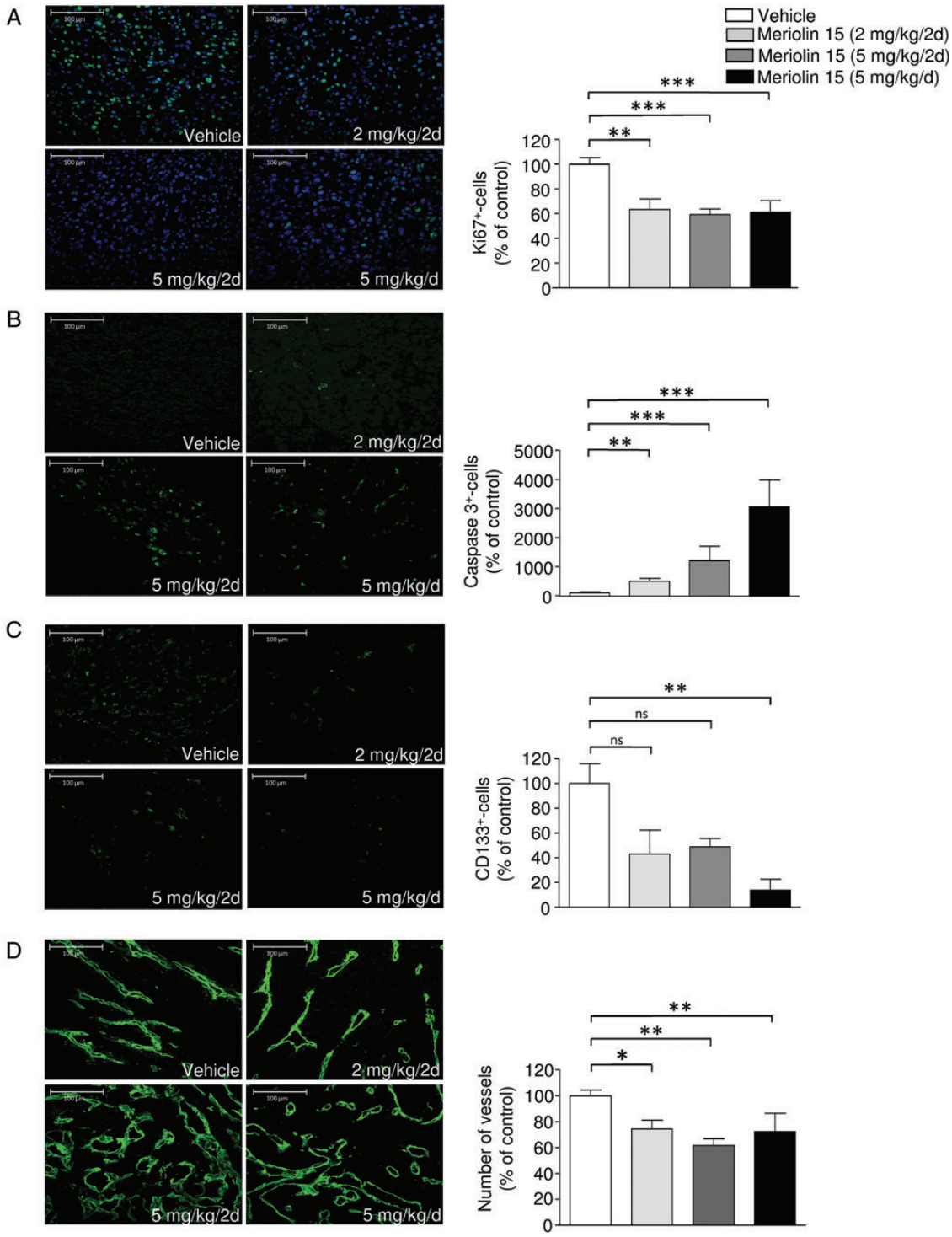

Fig. 7. In situ analysis of the proliferation rate, differentiation, apoptosis, and vascular content of U87-bearing tumoral sections from intraperitoneally treated mice. Immunostaining and quantitative analysis of the effect of meriolin 15 (2 mg/kg/2d, 5 mg/kg/2d, 5 mg/kg/d) on (A) cell proliferation using Ki67, (B) apoptosis using caspase 3, (C) stem cell numbers using CD133, and (D) vascularization using collagen IV antibodies in U87 xenografts. Immunostaining was performed on tumors at the end stage of experiment. Statistical significance was determined by the Kruskal-Wallis test followed by the Dunn post hoc test. $^{*}P < .05$; $^{**}P < .01$; $^{***}P < .001$ meriolin 15 groups versus vehicle group.

double impact of this new series of CDK inhibitors on both glial tumor and vascular compartments, it may represent a key targeted treatment for high-grade malignant glioma.

In vivo, meriolin 15 was investigated in a subcutaneous implanted xenograft model of U87 glioblastoma cells in which various oncogenes have been shown to be activated or

overexpressed,[49] a process classically used to test the antitumor activity of a number of cell cycle disruptors and antiangiogenic-targeted therapies. In a previous study, meriolin 3 had been shown to exhibit antitumoral activity on A4573 Ewing's sarcoma and LS174T colorectal carcinoma xenografted in nude mice.[23] A significant antitumor effect of meriolin 15 was detected during the first week of treatment and appeared to be enhanced by increasing the dose and the frequency of administration. However, systemic toxicity was observed at doses greater than 5 mg/kg/day. We tested a secondary model in which GBM was xenografted into nude mice, and a daily infusion schedule of meriolin 15 diluted in DMSO delayed tumor volume development and/or even led to tumor disappearance. The proper effect of DMSO on glioma growth in vivo is not surprising since this adjuvant has been found to suppress proliferation of mouse breast cancer cells,[55] arrest the cell cycle of lymphoid cell lines,[56,57] and provoke leukemia cellular differentiation leading to the disappearance of proliferation properties.[58,59] However, the sustained inhibition of human GBM sc1 growth after the end of the treatment period clearly indicates the direct long-term impact of meriolin 15 on glioma cell death.

Immunohistochemical analysis of treated tumors indicates that in vivo i.p. administration of meriolin 15 triggers a dose-dependent inhibition of glioma cell proliferation (decreased number of Ki67-positive cells), activation of the proapoptotic cascade (increased number of caspase 3-positive cells), and reduces detection of undifferentiated/glioma stem cells (less expression of the specific CD133 marker). Because CD133-expressing tumoral stem cells appear to be resistant to radiation therapy and chemotherapy and are therefore likely contribute to tumor recurrence and relapse,[60] meriolins may constitute a beneficial therapy via their antiproliferative and proapoptotic actions and through tumoral stem cell differentiation and/or death.

There is increasing evidence to support the concept of a microvascular niche in brain tumors where tumoral stem cells likely reside in close proximity to endothelial cells.[61] Interestingly, a recent work reported a decrease in stem cell numbers when tumors were treated with antiangiogenic agents, suggesting a direct impact of the specialized vascular compartment on tumoral stem cell survival.[62] Accordingly, the meriolin 15-induced disappearance of CD133-positive cells in xenografted U87 tumors suggests an in vivo antiangiogenic effect of these CDK inhibitors. In the meriolin 15-treated glioblastoma, we observed abundant type IV collagen immunoreactive basement membrane sleeves that resembled blood vessels with interconnection to survival vascular structures. Part of the difficulty in interpretation comes from incomplete knowledge of how antiangiogenic factors affect blood vessels. Strictly speaking, neo-angiogenic inhibitors block the growth of new blood vessels from existing vessels, but they also initiate regression and normalization of others.[63] As already described in tumors treated with VEGF inhibitors,[64] sleeves of type IV collagen have been shown to be particularly dense, whereas endothelial cells have degenerated. Here, we observed that meriolin 15 decreased the total number of collagen-positive structures and enlarged the caliber of basement membrane. These structures did not colocalize with CD31-positive vascular compartments (data not shown). This suggests that meriolin 15 initiates regression of tumoral glioma vascular endothelium, a process previously observed during tumor vascular normalization following antiangiogenic therapies.[65–67]

Altogether, the marked in vitro and in vivo antitumoral activities of the new class of CDK inhibitors represented by meriolins, and meriolin 15 in particular, target malignant glioma cells and endothelial cells with cell cycle arrest and apoptosis induction and therefore might represent an interesting lead compound. However, the described characteristics of meriolin 15 in the present study suggest pan-CDK inhibitory properties of the molecule that regulates multiple pathways for inducing cell death in glioma. This may be advantageous in apoptotic-resistant glioblastoma, but the downside resides in the antiproliferative impact upon neonatal astrocytes and toxicities. In this context, the only possible clinical use for meriolin 15 in human glioma would be local administration after surgery. In particular, meriolin 15 should be administered through convection-enhanced delivery[68] to limit toxicities to surrounding normal tissues. However, the competing toxicities did not make meriolin 15 the compound of choice among the meriolin library for clinical usage. Consequently, we are currently refining our meriolin-lead compounds and evaluating their quantitative structure-activity relationships to identify the best drug candidate. The issues involved in developing the optimal meriolin derivative are evaluation of the blood-brain barrier's permeability, the acquired less-toxic effects toward normal tissues, and the possible efficient combination with other chemotherapeutic agents as temozolomide and/or radiotherapy.

Authors' contributions

M.J., C.L., C.M., M.-T.S., and N.L. performed all the experiments (cell growth assays, cell cycle analysis, apoptosis, heterotopic xenografts, immunohistochemistry, and in vitro Sc1 experiments). L.D. and V.L. contributed to the heterotopic xenograft experiments and analysis. F.L., G.L. and B.J. synthesized meriolins. L.M. provided the background on meriolins, co-supervised the project (in particular the Mcl-1 and Myc sections), and contributed to the writing of the paper. J.H., P.G., and H.C. supervised the study and contributed to the writing of the paper.

Funding

This work was supported by Inserm, ManRos Therapeutics, the National Institute on Cancer (INCA, GLIOMER project) (H.C., B.J., J.H., L.M.), Institute on Innovative and Biomedical Research (IRIB). This research was partly supported by an FP7-KBBE-2012 grant (BlueGenics) to L.M. The University of Rouen, M.J. and C.L. were recipients of a fellowship from the ministry.

Acknowledgments

We gratefully acknowledge Mr Sébastien Arthaud, Mr Arnaud Arabo, Mr David Thomas, Mrs Huguette Lemonnier and Mrs Marie-Eve Mayer for skillful technical assistance.

Conflict of interest statement: None declared.

References

1. Wen PY, Kesari S. Malignant Gliomas in Adults. *N Engl J Med*. 2008; 359(5):492–507.
2. Ostrom QT, Gittleman H, Farah P, et al. CBTRUS statistical report: primary brain and central nervous system. Tumors diagnosed in the United States in 2006–2010. *Neuro Oncol*. 2013;15(2):ii1–ii56.
3. Louis DN, Ohgaki H, Wiestler OD, et al. The 2007 WHO classification of tumours of the central nervous system. *Acta Neuropathol*. 2007; 114(2):97–109.
4. Shinojima N, Tada K, Shiraishi S, et al. Prognostic value of epidermal growth factor receptor in patients with glioblastoma multiforme. *Cancer Res*. 2003;63(20):6962–6970.
5. Wen PY, Brandes AA. Treatment of recurrent high-grade gliomas. *Curr Opin Neurol*. 2009;22(6):657–664.
6. Deshpande A, Sicinski P, Hinds PW. Cyclins and cdks in development and cancer: a perspective. *Oncogene*. 2005;24(17):2909–2915.
7. Malumbres M, Barbacid M. Cell cycle, CDKs and cancer: a changing paradigm. *Nat Rev Cancer*. 2009;9(3):153–166.
8. Jen J, Harper JW, Bigner SH, et al. Deletion of p16 and p15 genes in brain tumors. *Cancer Res*. 1994;54(24):6353–6358.
9. He J, Allen JR, Collins VP, et al. CDK4 amplification is an alternative mechanism to p16 gene homozygous deletion in glioma cell lines. *Cancer Res*. 1994;54(22):5804–5807.
10. Ichimura K, Schmidt EE, Goike HM, et al. Human glioblastomas with no alterations of the CDKN2A (p16INK4A, MTS1) and CDK4 genes have frequent mutations of the retinoblastoma gene. *Oncogene*. 1996;13(5):1065–1072.
11. Ueki K, Ono Y, Henson JW, et al. CDKN2/p16 or RB alterations occur in the majority of glioblastomas and are inversely correlated. *Cancer Res*. 1996;56(1):150–153.
12. Solomon DA, Kim J-S, Jean W, et al. Conspirators in a capital crime: co-deletion of p18INK4c and p16INK4a/p14ARF/p15INK4b in glioblastoma multiforme. *Cancer Res*. 2008;68(21):8657–8660.
13. Wiedemeyer R, Brennan C, Heffernan TP, et al. Feedback circuit among INK4 tumor suppressors constrains human glioblastoma development. *Cancer Cell*. 2008;13(4):355–364.
14. Comprehensive genomic characterization defines human glioblastoma genes and core pathways. *Nature*. 2008;455(7216): 1061–1068.
15. Parsons DW, Jones S, Zhang X, et al. An integrated genomic analysis of human glioblastoma multiforme. *Science*. 2008;321(5897): 1807–1812.
16. Galons H, Oumata N, Meijer L. Cyclin-dependent kinase inhibitors: a survey of recent patent literature. *Expert Opin Ther Pat*. 2010;20(3): 377–404.
17. Galons H. Introduction for the special issue on kinase inhibitors. *Eur J Med Chem*. 2013;61:1.
18. Shapiro GI. Cyclin-dependent kinase pathways as targets for cancer treatment. *J Clin Oncol*. 2006;24(11):1770–1783.
19. Noble MEM, Endicott JA, Johnson LN. Protein kinase inhibitors: insights into drug design from structure. *Science*. 2004;303(5665): 1800–1805.
20. Luke JJ, D'Adamo DR, Dickson MA, et al. The cyclin-dependent kinase inhibitor flavopiridol potentiates doxorubicin efficacy in advanced sarcomas: preclinical investigations and results of a phase I dose-escalation clinical trial. *Clin Cancer Res*. 2012;18(9): 2638–2647.
21. Dickson MA, Shah MA, Rathkopf D, et al. A phase I clinical trial of FOLFIRI in combination with the pan-cyclin-dependent kinase (CDK) inhibitor flavopiridol. *Cancer Chemother Pharmacol*. 2010; 66(6):1113–1121.
22. Lapenna S, Giordano A. Cell cycle kinases as therapeutic targets for cancer. *Nat Rev Drug Discov*. 2009;8(7):547–566.
23. Bettayeb K, Tirado OM, Marionneau-Lambot S, et al. Meriolins, a new class of cell death inducing kinase inhibitors with enhanced selectivity for cyclin-dependent kinases. *Cancer Res*. 2007;67(17): 8325–8334.
24. Echalier A, Bettayeb K, Ferandin Y, et al. Meriolins (3-(pyrimidin-4-yl)-7-azaindoles): synthesis, kinase inhibitory activity, cellular effects, and structure of a CDK2/cyclin A/meriolin complex. *J Med Chem*. 2008;51(4):737–751.
25. Franco LH, Joffé EB, Puricelli L, et al. Indole alkaloids from the tunicate Aplidium meridianum. *J Nat Prod*. 1998;61(9):1130–1132.
26. Perry NB, Ettouati L, Litaudon M, et al. Alkaloids from the Antarctic sponge Kirkpatrickia varialosa. I: Variolin B, a new antitumour and antiviral compound. *Tetrahedron*. 1994;50(13):3987–3992.
27. Trimurtulu G, Faulkner DJ, Perry NB, et al. Alkaloids from the antarctic sponge Kirkpatrickia varialosa. Part 2: Variolin A and N(3′)-methyl tetrahydrovariolin B. *Tetrahedron*. 1994;50(13):3993–4000.
28. Gompel M, Leost M, De Kier Joffe EB, et al. Meridianins, a new family of protein kinase inhibitors isolated from the ascidian Aplidium meridianum. *Bioorg Med Chem Lett*. 2004;14(7):1703–1707.
29. Simone M, Erba E, Damia G, et al. Variolin B and its derivate deoxy-variolin B: new marine natural compounds with cyclin-dependent kinase inhibitor activity. *Eur J Cancer*. 2005;41(15): 2366–2377.
30. Castel H, Diallo M, Chatenet D, et al. Biochemical and functional characterization of high-affinity urotensin II receptors in rat cortical astrocytes. *J Neurochem*. 2006;99(2):582–595.
31. Lefebvre T, Gonzalez BJ, Vaudry D, et al. Paradoxical effect of ethanol on potassium channel currents and cell survival in cerebellar granule neurons. *J Neurochem*. 2009;110(3):976–989.
32. Kroemer G, Reed JC. Mitochondrial control of cell death. *Nat Med*. 2000;6(5):513–519.
33. Taillandier L, Antunes L, Angioi-Duprez KS. Models for neuro-oncological preclinical studies: solid orthotopic and heterotopic grafts of human gliomas into nude mice. *J Neurosci Methods*. 2003;125(1–2):147–157.
34. Gasser UE, Hatten ME. Neuron-glia interactions of rat hippocampal cells in vitro: glial-guided neuronal migration and neuronal regulation of glial differentiation. *J Neurosci*. 1990;10(4):1276–1285.
35. Wang LC, Baird DH, Hatten ME, et al. Astroglial differentiation is required for support of neurite outgrowth. *J Neurosci*. 1994; 14(5 Pt 2):3195–3207.
36. Darzynkiewicz Z, Juan G, Li X, et al. Cytometry in cell necrobiology: analysis of apoptosis and accidental cell death (necrosis). *Cytometry*. 1997;27(1):1–20.
37. Ehrenberg B, Montana V, Wei MD, et al. Membrane potential can be determined in individual cells from the nernstian distribution of cationic dyes. *Biophys J*. 1988;53(5):785–794.
38. Galluzzi L, Vitale I, Vacchelli E, Kroemer G. Cell death signaling and anticancer therapy. *Front Oncol*. 2011;1:5.
39. Folmer F, Jaspars M, Dicato M, et al. Marine cytotoxins: callers for the various dances of death. *Gastroenterol Hepatol Bed Bench*. 2009;2: 34–50.
40. Weerasinghe P, Buja LM. Oncosis: an important non-apoptotic mode of cell death. *Exp Mol Pathol*. 2012;93(3):302–308.

41. Janmey PA. The cytoskeleton and cell signaling: component localization and mechanical coupling. *Physiol Rev*. 1998;78(3): 763–781.
42. Lakshman M, Subramaniam V, Jothy S. CD44 negatively regulates apoptosis in murine colonic epithelium via the mitochondrial pathway. *Exp Mol Pathol*. 2004;76(3):196–204.
43. Lockshin RA, Zakeri Z. Apoptosis, autophagy, and more. *Int J Biochem Cell Biol*. 2004;36(12):2405–2419.
44. Jaeschke H, Lemasters JJ. Apoptosis versus oncotic necrosis in hepatic ischemia/reperfusion injury. *Gastroenterology*. 2003;125(4): 1246–1257.
45. Hoa N, Myers MP, Douglass TG, et al. Molecular mechanisms of paraptosis induction: implications for a non-genetically modified tumor vaccine. *PLoS ONE*. 2009;4(2):e4631.
46. Bettayeb K, Oumata N, Echalier A, et al. CR8, a potent and selective, roscovitine-derived inhibitor of cyclin-dependent kinases. *Oncogene*. 2008;27(44):5797–5807.
47. Bettayeb K, Baunbæk D, Delehouze C, et al. CDK Inhibitors Roscovitine and CR8 Trigger Mcl-1 Down-Regulation and Apoptotic Cell Death in Neuroblastoma Cells. *Genes Cancer*. 2010;1(4): 369–380.
48. Cai D, Byth KF, Shapiro GI. AZ703, an imidazo[1,2-a]pyridine inhibitor of cyclin-dependent kinases 1 and 2, induces E2F-1-dependent apoptosis enhanced by depletion of cyclin-dependent kinase 9. *Cancer Res*. 2006;66(1):435–444.
49. Michaud K, Solomon DA, Oermann E, et al. Pharmacologic inhibition of cyclin-dependent kinases 4 and 6 arrests the growth of glioblastoma multiforme intracranial xenografts. *Cancer Res*. 2010; 70(8):3228–3238.
50. Pore N, Liu S, Haas-Kogan DA, et al. PTEN mutation and epidermal growth factor receptor activation regulate vascular endothelial growth factor (VEGF) mRNA expression in human glioblastoma cells by transactivating the proximal VEGF promoter. *Cancer Res*. 2003;63(1):236–241.
51. Ali MA, Choy H, Habib AA, et al. SNS-032 prevents tumor cell-induced angiogenesis by inhibiting vascular endothelial growth factor. *Neoplasia*. 2007;9(5):370–381.
52. Melillo G, Sausville EA, Cloud K, et al. Flavopiridol, a protein kinase inhibitor, down-regulates hypoxic induction of vascular endothelial growth factor expression in human monocytes. *Cancer Res*. 1999; 59(21):5433–5437.
53. Liebl J, Weitensteiner SB, Vereb G, et al. Cyclin-dependent kinase 5 regulates endothelial cell migration and angiogenesis. *J Biol Chem*. 2010;285(46):35932–35943.
54. Zahler S, Liebl J, Fürst R, et al. Anti-angiogenic potential of small molecular inhibitors of cyclin dependent kinases in vitro. *Angiogenesis*. 2010;13(3):239–249.
55. Oz ES, Aydemir E, Fışkın K. DMSO exhibits similar cytotoxicity effects to thalidomide in mouse breast cancer cells. *Oncol Lett*. 2012;3(4): 927–929.
56. Takase K, Sawai M, Yamamoto K, et al. Reversible G1 arrest induced by dimethyl sulfoxide in human lymphoid cell lines: kinetics of the arrest and expression of the cell cycle marker proliferating cell nuclear antigen in Raji cells. *Cell Growth Differ*. 1992;3(8):515–521.
57. Teraoka H, Mikoshiba M, Takase K, et al. Reversible G1 arrest induced by dimethyl sulfoxide in human lymphoid cell lines: dimethyl sulfoxide inhibits IL-6-induced differentiation of SKW6-CL4 into IgM-secreting plasma cells. *Exp Cell Res*. 1996;222(1):218–224.
58. Santos NC, Figueira-Coelho J, Martins-Silva J, et al. Multidisciplinary utilization of dimethyl sulfoxide: pharmacological, cellular, and molecular aspects. *Biochem Pharmacol*. 2003;65(7):1035–1041.
59. Collins SJ, Ruscetti FW, Gallagher RE, et al. Terminal differentiation of human promyelocytic leukemia cells induced by dimethyl sulfoxide and other polar compounds. *Proc Natl Acad Sci USA*. 1978;75(5): 2458–2462.
60. He J, Shan Z, Li L, et al. Expression of glioma stem cell marker CD133 and O6-methylguanine-DNA methyltransferase is associated with resistance to radiotherapy in gliomas. *Oncol Rep*. 2011;26(5): 1305–1313.
61. Calabrese C, Poppleton H, Kocak M, et al. A perivascular niche for brain tumor stem cells. *Cancer Cell*. 2007;11(1):69–82.
62. Folkins C, Man S, Xu P, et al. Anticancer therapies combining antiangiogenic and tumor cell cytotoxic effects reduce the tumor stem-like cell fraction in glioma xenograft tumors. *Cancer Res*. 2007;67(8):3560–3564.
63. McDonald DM, Choyke PL. Imaging of angiogenesis: from microscope to clinic. *Nat Med*. 2003;9(6):713–725.
64. Inai T, Mancuso M, Hashizume H, et al. Inhibition of vascular endothelial growth factor (VEGF) signaling in cancer causes loss of endothelial fenestrations, regression of tumor vessels, and appearance of basement membrane ghosts. *Am J Pathol*. 2004; 165(1):35–52.
65. Baluk P, Morikawa S, Haskell A, et al. Abnormalities of basement membrane on blood vessels and endothelial sprouts in tumors. *Am J Pathol*. 2003;163(5):1801–1815.
66. Baluk P, Hashizume H, McDonald DM. Cellular abnormalities of blood vessels as targets in cancer. *Curr Opin Genet Dev*. 2005;15(1): 102–111.
67. Verreault M, Strutt D, Masin D, et al. Vascular normalization in orthotopic glioblastoma following intravenous treatment with lipid-based nanoparticulate formulations of irinotecan (Irinophore C™), doxorubicin (Caelyx®) or vincristine. *BMC Cancer*. 2011;11:124.
68. Lopez KA, Waziri AE, Canoll PD, et al. Convection-enhanced delivery in the treatment of malignant glioma. *Neurol Res*. 2006;28(5): 542–548.